DALTON
FULL PAPER

Bridging ability of a novel polydentate ligand (H_2L) comprising an oxime function. Structures of a mononuclear precursor [NiL] and a dinuclear Cu^{II}_2 complex. Magnetic properties of mononuclear (Ni^{II} and Cu^{II}), dinuclear (Cu^{II}_2, Ni^{II}_2, $Ni^{II}Cu^{II}$ and $Cu^{II}Cr^{III}$) and trinuclear (Cu^{II}_3, $Cu^{II}Mn^{II}Cu^{II}$ and $Cu^{II}Zn^{II}Cu^{II}$) complexes‡

Jean-Pierre Costes,*,† Françoise Dahan, Arnaud Dupuis and Jean-Pierre Laurent

Laboratoire de Chimie de Coordination du CNRS, UPR 8241, liée par conventions à l'Université Paul Sabatier et à l'Institut National Polytechnique de Toulouse, 205 route de Narbonne, 31077 Toulouse Cedex, France

A novel non-symmetrical polydentate Schiff base ligand 3-({2-[(1-methyl-3-oxobut-1-enyl)amino]ethyl}imino)-butan-2-one oxime (H_2L) comprising an oxime function among various donor sites yields neutral [$Ni^{II}L$] and [$Cu^{II}L$] complexes. The structural determination of [NiL] confirms the deprotonation of the oxime function. The deprotonated oxime oxygen atom can react with auxiliary complexes to give homo- and hetero-di- and tri-nuclear entities. The structural determination of a homodinuclear copper complex clearly shows the presence of the expected oxime bridge, along with an unexpected ketonic bridge between the two copper centres leading to a Cu[O,NO]Cu core. A moderate antiferromagnetic interaction is present in the di- and tri-nuclear copper complexes. A similar interaction is also observed in the heteronuclear complexes ($Cu^{II}Ni^{II}$ and $Cu^{II}Mn^{II}$) and, more surprisingly, in the heterodinuclear $Cu^{II}Cr^{III}$ entity. A generalization of the Cu[O,NO]Cu structure leads to a justification of these magnetic properties.

In search of new polydentate bridging ligands we have been interested in designing a ligand (H_2L, Fig. 1) which comprises an oxime function among various donor sites.

Indeed it has been known for more than twenty years that oximato groups (=N–O^-) can bridge metal ions through their imino nitrogen and deprotonated oxygen atoms. Very generally double oximato bridges or association of a single N–O bridge with a second bridging ligand are involved in the resulting bi- or poly-nuclear complexes. Many types of homo- and hetero-polynuclear complexes[1–15] have been obtained and magnetic investigations have revealed a great variety of behaviours, strong antiferromagnetism, weak antiferromagnetism and even ferromagnetism. It may be noted that singlet–triplet energy gaps of the order of 1000 cm^{-1} have been reported for oximato bridged dinuclear copper(II) complexes in which the double oximato bridge adopts the *cis* conformation.[3,10,11]

The present paper reports on the preparation, characterization and magnetic study of mononuclear Cu^{II} and Ni^{II}, dinuclear complexes involving the $Cu^{II}Cu^{II}$, $Cu^{II}Ni^{II}$ and $Cu^{II}Cr^{III}$ pairs and trinuclear complexes $Cu^{II}Cu^{II}Cu^{II}$, $Cu^{II}Zn^{II}Cu^{II}$ and $Cu^{II}Mn^{II}Cu^{II}$ deriving from H_2L. The structures of a mononuclear [NiL] precursor and a homodinuclear Cu^{II}_2 complex are also reported.

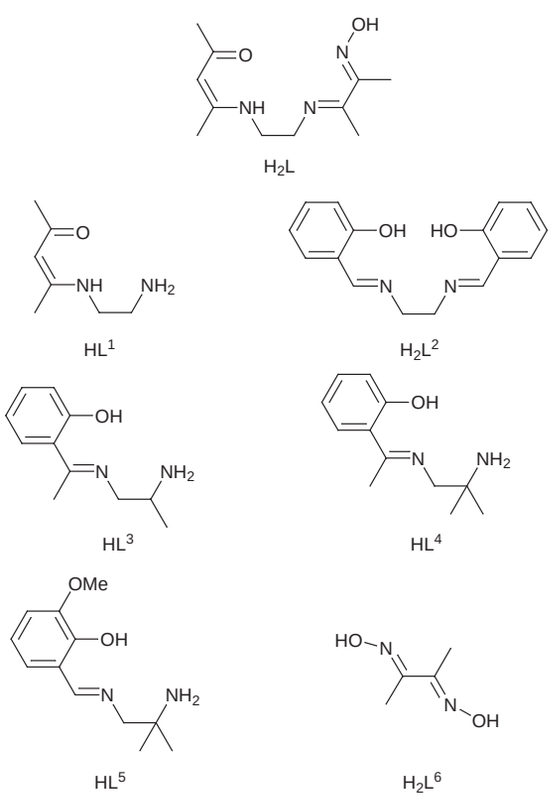

Fig. 1 Schematic representation of ligands used in this work

Experimental

All starting materials were purchased from Aldrich and were used without further purification. Elemental analyses (C, H, N) were carried out by the Service de Microanalyse du Laboratoire de Chimie de Coordination, Toulouse. Fourier transform infrared spectroscopy on KBr pellets was performed on a Perkin-Elmer 1725 X FT-IR instrument. ^1H and ^{13}C NMR spectra were recorded at ambient temperature (295 K) with Bruker AC200 or Bruker WM250 spectrometers. 2-D ^1H COSY experiments using standard programs and 2-D pulse-field gradient HMQC ^1H–^{13}C correlation using the PFG-HMQC standard program were performed on a Bruker AMX400 spectrometer. All chemical shifts (^1H and ^{13}C) are given in ppm *versus* $SiMe_4$ using CD_3COCD_3, $CDCl_3$ or [$^2H_6$]dmso as solvents. Electronic spectra were obtained with a Cary 2390

† E-Mail: costes@lcc-toulouse.fr

‡ *Non SI-unit employed:* $\mu_B \approx 9.27 \times 10^{-24}$ J T^{-1}.

spectrometer. Mass spectra (FAB^+) were recorded in dmf or dmso as solvents and 3-nitrobenzyl alcohol matrix with a Nermag R10-10 spectrometer. Magnetic susceptibility data were collected on powdered samples of the different compounds with use of a SQUID-based sample magnetometer on a QUANTUM Design Model MPMS instrument. All data were corrected for diamagnetism of the ligands estimated from Pascal's constants.[16] EPR spectra were recorded at X-band frequency (9.4–9.5 GHz) with a Bruker ESP 300E spectrometer.

CAUTION: Some complexes reported in the following were isolated as perchlorate salts. We worked with these complexes in a number of organic solvents without any incident, and, as solids, they seem to be reasonably stable to shock and heat. In spite of these observations, the unpredictable behaviour of perchlorate salts[17] necessitates extreme care in their handling.

Synthesis of the ligands and complexes

Ligand H_2L, 3-({2-[(1-methyl-3-oxobut-1-enyl)amino]ethyl}-imino)butan-2-one oxime. Butanedione monoxime was added to an ethanolic solution (50 ml) of HL[1] [18] (5 g, 3.5×10^{-2} mol). The solution was stirred at ambient temperature for 24 h. The resulting precipitate was filtered off, washed with a little cold ethanol and then with diethyl ether. Yield: 4.4 g, 55% (Found: C, 58.9; H, 8.6; N, 18.8. Calc. for $C_{11}H_{19}N_3O_2$: C, 58.6; H, 8.5; N, 18.7%). M.p. 162 °C. ^{1}H NMR (250 MHz, 20 °C, $CDCl_3$), δ 1.956, 1.976, 1.994, 2.068 (s, CH_3), 3.536–3.642 (m, CH_2), 4.954 (s, CH), 5.153 (br, NOH), 10.924 (br, NH). ^{13}C-{^{1}H} NMR (62.89 MHz, 20 °C, $CDCl_3$), δ 9.07 (*C*H_3C=NOH), 13.67 (*C*H_3C=N), 19.18 (*C*H_3CNH), 28.63 (*C*H_3C=O), 43.85 (CH_2NH), 51.74 (CH_2N), 95.44 (CH), 158.62, 163.58, 166.22 (C=N), 194.92 (C=O).

[Ni(HL)]ClO_4 1. Nickel perchlorate (1.6 g, 4.4×10^{-3} mol) in methanol (20 ml) was added to a stirred solution of H_2L (1 g, 4.4×10^{-3} mol) in methanol (30 ml). The orange-yellow precipitate that quickly appeared was filtered off, washed with methanol and diethyl ether. Yield: 1.4 g, 80% (Found: C, 32.7; H, 5.0; N, 10.5. Calc. for $C_{11}H_{18}ClN_3NiO_6 \cdot H_2O$: C, 33.0; H, 5.0; N, 10.5%).

[Cu(HL)]Cl 2. Copper chloride (0.3 g, 2.2×10^{-3} mol) in methanol (10 ml) was added to a stirred solution of H_2L (0.5 g, 2.2×10^{-3} mol) in methanol (10 ml). The green solution was concentrated after 1 h yielding a green precipitate which was filtered off and dried. Yield: 0.35 g, 45% (Found: C, 37.7; H, 6.3; N, 12.0. Calc. for $C_{11}H_{18}ClCuN_3O_2 \cdot 1.5H_2O$: C, 37.7; H, 6.0; N, 12.0%). UV/VIS: λ_{max} = 630 nm (pyridine). EPR (MeOH, 300 K) g_{iso} = 2.105, A_{iso} = 77 G, $A_{N\ iso}$ = 14.5 G.

[NiL] 3. Addition of triethylamine (0.2 ml, 1.4×10^{-3} mol) to [Ni(HL)]ClO_4 (0.5 g, 1.2×10^{-3} mol) dissolved in acetone (15 ml) induced a colour change and, a few minutes later, precipitation of a red complex which was filtered off, washed with acetone and diethyl ether. Yield: 0.33 g, 95% (Found: C, 46.5; H, 6.2; N, 15.1. Calc. for $C_{11}H_{17}N_3NiO_2$: C, 46.9; H, 6.1; N, 14.9%). ^{1}H NMR (400 MHz, 20 °C, $CDCl_3$), δ 1.831 (s, CH_3C=NO), 1.919 (s, C*H*$_3$C=CH), 1.959 (s, CH_3C=N), 1.997 (s, CH_3C=O), 3.477 (t, J = 6.5 Hz, CH_2NCCNO), 3.681 (t, J = 6.5 Hz, C*H*$_2$NCCH), 4.970 (s, CH). ^{13}C-{^{1}H} NMR (100.62 MHz, 20 °C, $CDCl_3$), δ 10.92 (*C*H_3C=NO), 15.27 (*C*H_3C=N), 20.77 (*C*H_3C=CH), 25.35 (*C*H_3C=O), 50.33 (*C*H_2NCCNO), 56.08 (*C*H_2NCCH), 100.39 (CH), 149.51 (C=NO), 165.52 (N*C*=CH), 170.77 (N=*C*C=NO), 178.07 (C=O). A CH_2Cl_2 solution kept at room temperature provided orange red crystals which were filtered off and air-dried.

[CuL] 4. To a stirred solution of H_2L (0.5 g, 2.2×10^{-3} mol) in ethanol (15 ml) was first added copper chloride (0.3 g, 2.2×10^{-3} mol) and then triethylamine (0.36 ml, 2.5×10^{-3} mol). The mixture was heated for a few min and a purple precipitate began to appear after 2 h. It was collected by filtration and washed with a little ethanol and diethyl ether. Yield: 0.2 g, 31% (Found: C, 46.1; H, 6.1; N, 14.6. Calc. for $C_{11}H_{17}CuN_3O_2$: C, 46.1; H, 6.0; N, 14.7%). UV/VIS: λ_{max} = 525 nm (CH_2Cl_2); 570 nm (pyridine). EPR (CH_2Cl_2, 300 K) g_{iso} = 2.082, A_{iso} = 95 G, $A_{N\ iso}$ = 14.5 G.

[NHEt$_3$][CuL]Cl. To a stirred solution of H_2L (0.5 g, 2.2×10^{-3} mol) in acetone (15 ml) was first added copper chloride (0.3 g, 2.2×10^{-3} mol) and, a few minutes later, triethylamine (0.36 ml, 2.5×10^{-3} mol). The mixture was heated for 5 min, giving a purple precipitate which was collected by filtration and washed with acetone and diethyl ether. Yield: 0.9 g, 90% (Found: C, 48.7; H, 8.1; N, 12.4. Calc. for $C_{17}H_{33}ClCuN_4O_2 \cdot 0.5C_2H_6O$: C, 49.0; H, 7.9; N, 12.4%). UV/VIS: λ_{max} = 526 nm (CH_2Cl_2).

[Hpip][CuL]Cl. Use of piperidine (pip) instead of triethylamine yielded [Hpip][CuL]Cl. Yield: 0.9 g, 92% (Found: C, 47.6; H, 7.5; N, 13.0. Calc. for $C_{16}H_{29}ClCuN_4O_2 \cdot 0.5C_2H_6O$: C, 48.0; H, 7.3; N, 12.8%). UV/VIS: λ_{max} = 525 nm (MeOH).

[{CuL^3(O$_2$CMe)}$_2$]. Hydroxyacetophenone (1.36 g, 1×10^{-2} mol) and 1,2-diaminopropane (0.74 g, 1×10^{-2} mol) were stirred overnight in ethanol (50 ml). Copper acetate (2.0 g, 1×10^{-2} mol) was added as a solid under stirring at ambient temperature. One hour later, the mixture was filtered off and the filtrate was concentrated with a rotating evaporator, leaving a blue paste. Addition of acetone to the paste and stirring gave a blue precipitate which was filtered off and washed with acetone and diethyl ether. Yield: 2.1 g, 65% (Found: C, 50.2; H, 5.7; N, 8.7. Calc. for $C_{13}H_{18}CuN_2O_3$: C, 49.8; H, 5.7; N, 8.9%). UV/VIS: λ_{max} = 565 nm (CH_2Cl_2).

[(CuL^4)$_3$(OH)][ClO_4]$_2$. Hydroxyacetophenone (0.7 g, 5.1×10^{-3} mol) and 2-methyl-1,2-diaminopropane (0.45 g, 1×10^{-2} mol) in ethanol (20 ml) were stirred and heated for 20 min. Then copper perchlorate (1.9 g, 5.1×10^{-3} mol) was added and, 2 h later, triethylamine (0.7 ml, 9.9×10^{-3} mol). The green precipitate which appeared was filtered off, washed with ethanol. Yield: 1 g, 54% (Found: C, 39.3; H, 5.4; N, 7.6. Calc. for $C_{36}H_{52}Cl_2Cu_3N_6O_{12} \cdot 4H_2O$: C, 39.5; H, 5.5; N, 7.7%). UV/VIS: λ_{max} = 605 nm (MeOH).

[CuL^5(py)]ClO_4. To a stirred solution of 3-methoxysalicylaldehyde (1.52 g, 1×10^{-2} mol) in methanol (50 ml) was first added copper perchlorate (3.7 g, 1×10^{-2} mol) dissolved in water (10 ml) and then pyridine (1.6 g, 2×10^{-2} mol). A few minutes later, a methanolic solution (10 ml) of 2-methyl-1,2-diaminopropane (0.9 g, 1×10^{-2} mol) was added at once with stirring at ambient temperature. The precipitate was filtered off after 2 h and washed with cold methanol and diethyl ether. Yield: 3.3 g, 72% (Found: C, 43.7; H, 4.5; N, 8.9. Calc. for $C_{17}H_{22}ClCuN_3O_6$: C, 44.1; H, 4.7; N, 9.1%). UV/VIS: λ_{max} = 575 nm (CH_2Cl_2).

[LNiNiL^3]ClO_4 5. A mixture of [NiL] (0.11 g, 3.9×10^{-4} mol) and [{NiL^3(O$_2$CMe)}$_2$] (0.12 g, 3.9×10^{-4} mol)[19] was stirred at ambient temperature in methanol (10 ml) with sodium perchlorate (0.1 g, 8.1×10^{-4} mol). The precipitate was isolated after 2 h by filtration and washed with methanol and diethyl ether. Yield: 0.17 g, 69% (Found: C, 41.4; H, 4.9; N, 10.9. Calc. for $C_{22}H_{32}ClN_5Ni_2O_7$: C, 41.8; H, 5.1; N, 11.1%). Mass spectrum (FAB^+): m/z = 530 (100), $[C_{22}H_{32}N_5Ni_2O_3]^+$.

[LNiCuL^3]ClO_4 6. A similar experimental procedure starting with [NiL] (0.13 g, 4.6×10^{-4} mol) and [{CuL^3(O$_2$CMe)}$_2$] (0.15 g, 4.6×10^{-4} mol) yielded the desired product (0.21 g, 68%) (Found: C, 41.4; H, 4.8; N, 10.8. Calc. for $C_{22}H_{32}ClCuN_5NiO_7$: C, 41.5; H, 5.1; N, 11.0%). Mass spectrum (FAB^+):

m/z = 535 (100), $[C_{22}H_{32}ClCuN_5NiO_3]^+$. UV/VIS: λ_{max} = 530 nm (MeOH).

[LCuNiL^3]ClO$_4$ 7. Use of [CuL] (0.14 g, 4.8×10^{-4} mol) and [{NiL^3(O$_3$CMe)}$_2$] (0.15 g, 4.8×10^{-4} mol) with the stoichiometric amount of $NaClO_4$ (0.6 g, 4.8×10^{-4} mol) in methanol (10 ml) and at ambient temperature gave a product which was precipitated by addition of diethyl ether (10 ml). Yield: 0.15 g, 50% (Found: C, 41.1; H, 4.9; N, 10.9. Calc. for $C_{22}H_{32}ClCuN_5NiO_7$: C, 41.5; H, 5.1; N, 11.0%). Mass spectrum (FAB$^+$): m/z = 535 (100), $[C_{22}H_{32}CuN_5NiO_3]^+$. UV/VIS: λ_{max} = 525 nm (MeOH).

[LCuCuL^3]ClO$_4$ 8. The complexes [Hpip][CuL]Cl (0.2 g, 4.6×10^{-4} mol) and [{CuL^3(O$_2$CMe)}$_2$] (0.15 g, 4.6×10^{-4} mol) were mixed and stirred at ambient temperature in methanol (8 ml) with sodium perchlorate (0.1 g, 8.1×10^{-4} mol). The solution was reduced to half volume after 3 h and filtered giving a purple precipitate which was washed with cold methanol and diethyl ether. Yield: 0.16 g, 54% (Found: C, 41.7; H, 5.0; N, 10.6. Calc. for $C_{22}H_{32}ClCu_2N_5O_7$: C, 41.2; H, 5.0; N, 10.9%). Mass spectrum (FAB$^+$): m/z = 540 (87), $[C_{22}H_{32}Cu_2N_5O_3]^+$. UV/VIS: λ_{max} = 530 nm (CH_2Cl_2); 540 nm (MeOH). Suitable crystals for X-ray analysis were obtained by slow evaporation of a MeOH solution at room temperature. A similar procedure, starting with [(CuL^4)$_3$(OH)][ClO$_4$]$_2$ or [CuL^5(py)]ClO$_4$ and [Hpip][CuL]Cl yielded the desired complexes.

[LCuCuL^4]ClO$_4$ 9. Yield: 0.15 g, 50% (Found: C, 41.7; H, 4.9; N, 10.5. Calc. for $C_{23}H_{34}ClCu_2N_5O_7$: C, 42.2; H, 5.2; N, 10.7%). Mass spectrum (FAB$^+$): m/z = 554 (75), $[C_{23}H_{34}Cu_2N_5O_3]^+$. UV/VIS: λ_{max} = 535 nm (CH_2Cl_2).

[LCuCuL^5]ClO$_4$ 10. Yield: 0.10 g, 35% (Found: C, 41.2; H, 5.0; N, 10.3. Calc. for $C_{23}H_{34}ClCu_2N_5O_8$: C, 41.2; H, 5.1; N, 10.4%). Mass spectrum (FAB$^+$): m/z = 570 (67), $[C_{23}H_{34}Cu_2N_5O_4]^+$. UV/VIS: λ_{max} = 535 nm (CH_2Cl_2).

[LCuCu(HL^6)$_2$] 11. The complexes [CuL] (0.07 g, 2.4×10^{-4} mol) and [Cu(HL^6)$_2$] (0.07 g, 2.4×10^{-4} mol) in dichloromethane (10 ml) were stirred and heated for 10 min. Addition of diethyl ether to the cooled solution yielded a precipitate which was filtered off and washed with diethyl ether. Yield: 0.12 g, 85% (Found: C, 38.9; H, 5.1; N, 16.6. Calc. for $C_{19}H_{31}Cu_2N_7O_6$: C, 39.3; H, 5.3; N, 16.9%). UV/VIS: λ_{max} = 525 nm (MeOH).

[Cu(CuL)$_2$][ClO$_4$]$_2$·2H$_2$O 12. A mixture of [Hpip][CuL]Cl (0.12 g, 2.7×10^{-4} mol) with a slight excess of Cu(ClO$_4$)$_2$·6H$_2$O (0.08 g, 2.1×10^{-4} mol) in ethanol (10 ml) was stirred at ambient temperature for 2 h, giving a brown precipitate which was filtered off and washed with ethanol and diethyl ether. Yield: 0.06 g, 52% (Found: C, 30.0; H, 4.2; N, 9.3. Calc. for $C_{22}H_{34}Cl_2Cu_3N_6O_{12}·2H_2O$: C, 30.3; H, 4.4; N, 9.6%). Mass spectrum (FAB$^+$): m/z = 734 (10), $[C_{22}H_{34}ClCu_3N_6O_8]^+$. UV/VIS: λ_{max} = 520 nm (MeOH).

[Zn(CuL)$_2$][ClO$_4$]$_2$·2H$_2$O 13. This complex was prepared as described above, using Zn(ClO$_4$)$_2$·6H$_2$O instead of Cu(ClO$_4$)$_2$·6H$_2$O. Yield: 60% (Found: C, 33.8; H, 4.4; N, 9.5. Calc. for $C_{22}H_{34}Cl_2Cu_2N_6O_{12}Zn·C_3H_6O$: C, 33.5; H, 4.5; N, 9.4%). Mass spectrum (FAB$^+$): m/z = 735 (13), $[C_{22}H_{34}ClCu_2N_6O_8Zn]^+$. UV/VIS: λ_{max} = 525 nm (MeOH).

[LCuCrL^2](NO$_3$)·H$_2$O 14. A solution of [CuL] (0.07 g, 2.4×10^{-4} mol) and of [CrL^2(NO$_3$)]·2H$_2$O[20] (0.1 g, 2.4×10^{-4} mol) in methanol (10 ml) was stirred for 2 h. Addition of diethyl ether yielded a brown precipitate which was filtered off and washed with diethyl ether. Yield: 0.1 g, 60% (Found: C, 47.0; H, 4.7; N, 12.0. Calc. for $C_{27}H_{31}CrCuN_6O_7·H_2O$: C, 47.3; H, 4.8; N, 12.3%). Mass spectrum (FAB$^+$): m/z = 604 (100), $[C_{27}H_{31}CrCuN_5O_4]^+$. UV/VIS: λ_{max} = 525 nm (MeOH).

[(CuL)$_2$Mn(bipy)][ClO$_4$]$_2$·3H$_2$O 15. To [Hpip][CuL]Cl (0.12 g, 2.7×10^{-4} mol) in methanol was added Mn(ClO$_4$)$_2$·6H$_2$O (0.09 g, 2.7×10^{-4} mol) and bipy (0.09 g, 5.5×10^{-4} mol). The mixture was stirred for 30 min and then filtered off, giving a red violet precipitate which was washed with methanol and diethyl ether. Yield: 0.12 g, 90% (Found: C, 36.9; H, 4.7; N, 10.6. Calc. for $C_{32}H_{42}Cl_2Cu_2MnN_8O_{12}·3H_2O$: C, 37.0; H, 4.6; N, 10.8%). Mass spectrum (FAB$^+$): m/z = 882 (7), $[C_{32}H_{42}ClCu_2MnN_8O_8]^+$, 726 (100), $[C_{22}H_{34}ClCu_2MnN_6O_8]^+$. UV/VIS: λ_{max} = 525 (MeOH).

X-Ray crystallography

Crystals of compounds **3** and **8** were mounted on a CAD4 Enraf-Nonius four-circle diffractometer using a graphite crystal monochromator [λ(Mo-Kα) = 0.710 73 Å]. The temperature of measurement was 293 K. The reflections were corrected for Lorentz-polarisation effects and for absorption with the MolEN package.[21] The structures were solved using a Patterson procedure with the SHELXS 86 program[22] and refined against all F^2 (SHELXL 93)[23] with a weighting scheme $w^{-1} = \sigma^2(F^2) + (aP)^2 + bP$ where $3P = (2F_c^2 + F_o^2)$ and a and b are constants adjusted by the program.

Crystal data for complex 3. $C_{11}H_{17}N_3NiO_2$, M = 281.99, monoclinic, space group $P2_1/n$ (no. 14), a = 7.247(1), b = 11.224(1), c = 14.696(1) Å, β = 96.63(2)°, U = 1187.4(2) Å^3 (by least-squares refinement on diffractometer angles from 25 centred reflections, $18 < 2\theta < 34°$), Z = 4, D_c = 1.577 Mg m^{-3}, $F(000)$ = 592, orange-red needle with dimensions 0.50 × 0.15 × 0.05 mm, μ = 1.627 mm^{-1}. 2508 Reflections measured by ω–2θ scans in the range $3 < 2\theta < 52°$, $+h$, $+k$, $\pm l$, no significant intensity standards variations, gaussian absorption corrections,[24] transmission factors 0.33–0.61, 2322 independent reflections (R_{int} = 0.0177). All non-hydrogen atoms were refined with anisotropic thermal parameters. Hydrogen atoms were included using a riding model. The final $wR(F^2)$ was 0.0532 for all 2322 F^2 and the conventional $R(F)$ was 0.0238 [for 1262 $F > 4\sigma(F)$] for 154 parameters, GOF = 0.889, maximum Δ/σ = 0.001, $\Delta\rho_{max}$ = 0.193, $\Delta\rho$ = −0.181 e Å^{-3}.

Crystal data for complex 8. $C_{22}H_{32}ClCu_2N_5O_7$, M = 641.07, monoclinic, space group $P2_1/c$ (no. 14), a = 13.401(2), b = 9.582(2), c = 22.149(3) Å, β = 107.26(2)°, U = 2716.0(7) Å^3 (by least-squares refinement on diffractometer from 25 centred reflections, $24 < 2\theta < 30°$), Z = 4, D_c = 1.568 Mg m^{-3}, $F(000)$ = 1320, dark-red parallelepiped with dimensions 0.50 × 0.50 × 0.20 mm, μ = 1.680 mm^{-1}. 6139 Reflections measured by ω–2θ scans in the range $3 < 2\theta < 54°$, $+h$, $+k$, $\pm l$, no significant intensity standards variations, semi-empirical absorption corrections[25] based on ψ scans, transmission factors 0.72–1.00, 5898 independent reflections (R_{int} = 0.0123). All non-hydrogen atoms were refined with anisotropic thermal parameters. Hydrogen atoms were included using a riding model. The final $wR(F^2)$ was 0.0874 for all 5898 F^2 and the conventional $R(F)$ was 0.0314 [for 4495 $F > 4\sigma(F)$] for 334 parameters, GOF = 0.960, maximum Δ/σ = 0.005, $\Delta\rho_{max}$ = 0.275, $\Delta\rho_{min}$ = −0.0317 e Å^{-3}.

CCDC reference number 186/922.

See http://www.rsc.org/suppdata/dt/1998/1307/ for crystallographic files in .cif format.

Results and Discussion

Synthesis and general characterization of the ligand and mononuclear complexes

The free unsymmetrical Schiff base ligand 3-({2-[(1-methyl-3-oxobut-1-enyl)amino]ethyl}imino)butan-2-one oxime (H_2L) is readily obtained by reacting equimolar amounts of 4-[(2-aminoethyl)amino]pent-3-en-2-one (HL^1)[18] and butanedione

Table 1 Selected bond lengths (Å) and angles (°) for compound **3**

Ni–O(1)	1.828(2)	Ni–N(1)	1.842(2)
Ni–N(2)	1.811(2)	Ni–N(3)	1.894(2)
O(1)–Ni–N(1)	97.07(9)	N(1)–Ni–N(2)	86.20(9)
O(1)–Ni–N(2)	176.73(8)	N(1)–Ni–N(3)	168.99(9)
O(1)–Ni–N(3)	93.69(9)	N(2)–Ni–N(3)	83.06(9)

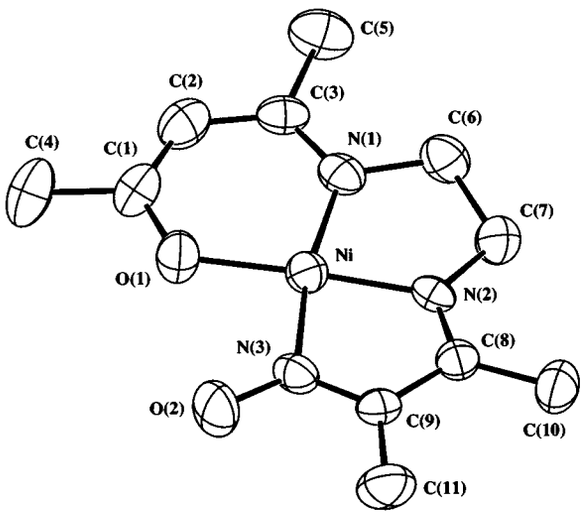

Fig. 2 Molecular plot of **3** with ellipsoids drawn at the 50% probability level

monoxime in ethanol or in diisopropyl ether with yields of 50 to 55%. It has been characterized by analysis and NMR which is an appropriate technique to evidence its unsymmetrical character through the non-equivalence of the CH_2 groups of the diamino chain, along with the presence of signals coming from the pentanedione and the butanedione monoxime moieties.

The best route to the mononuclear complexes depends on the metal considered. In the case of nickel, adding nickel perchlorate to a stirred solution of the ligand in methanol quickly gives an orange voluminous precipitate which analyses as $[Ni(HL)]ClO_4$ **1** and contains a protonated oxime function. Addition of triethylamine to an acetone solution of $[Ni(HL)]ClO_4$ yields a red precipitate which analyses as the neutral complex [NiL] **3**. Although the same processes allow the isolation of the related copper complexes **2** and **4**, better yields are obtained through the use of $[NHEt_3][CuL]Cl$ or [Hpip][CuL]Cl which are easily obtained by addition of a base (triethylamine or piperidine) to a mixture of equimolar amounts of H_2L and $CuCl_2$ in acetone.

Precise information concerning the nature of the copper complexes **2** and **4** is afforded by EPR spectroscopy. The powdered spectra which display a broad signal centered at *ca.* $g = 2.06$ are uninformative but the solution spectra of both complexes at $T = 300$ K point out seven superhyperfine (shf) lines superimposed on the hyperfine structure indicating that the environment of the copper ion comprises three nitrogen atoms (^{14}N, $I = 1$) and implying that the oxygen atom of the oxime group is not involved in the co-ordination sphere.

This conclusion is supported for [NiL] **3** by a structural determination. The structure consists of neutral [NiL] entities without any solvent molecule. A molecular plot[26] is shown in Fig. 2, whereas relevant bond distances and angles are listed in Table 1. The nickel ion has a slightly distorted square-planar co-ordination and is surrounded by three nitrogen and one oxygen atoms from the ligand L so that the oxygen atom of the oxime function remains uncomplexed. The 6, 5, 5-chelate ring arrangement around the central nickel atom introduces a deviation of the N(1)–Ni–N(3) angle from 180° [168.99(9)°] which reflects the residual strain in the ligand resulting from co-ordination to the metal. The five-membered ring formed by the diamine moiety chelating the nickel ion has a λ *gauche* conformation. There is no evidence for intramolecular hydrogen bonds.

Table 2 Selected bond lengths (Å) and angles (°) for compound **8**

Cu(1)–O(1)	1.881(2)	Cu(2)–O(2)	1.872(2)
Cu(1)–N(1)	1.913(2)	Cu(2)–O(3)	1.965(2)
Cu(1)–N(2)	1.917(2)	Cu(2)–N(4)	1.963(2)
Cu(1)–N(3)	1.996(2)	Cu(2)–N(5)	1.985(2)
		Cu(2)–O(1)	2.524(2)
O(1)–Cu(1)–N(1)	97.43(9)	O(2)–Cu(2)–O(3)	89.29(8)
O(1)–Cu(1)–N(2)	174.44(9)	O(2)–Cu(2)–N(4)	93.07(9)
O(1)–Cu(1)–N(3)	96.93(8)	O(2)–Cu(2)–N(5)	171.08(12)
N(1)–Cu(1)–N(2)	84.95(10)	O(3)–Cu(2)–N(4)	167.79(10)
N(1)–Cu(1)–N(3)	165.64(9)	O(3)–Cu(2)–N(5)	91.06(9)
N(2)–Cu(1)–N(3)	80.78(9)	N(4)–Cu(2)–N(5)	84.76(10)
		O(2)–Cu(2)–O(1)	98.99(10)
		O(3)–Cu(2)–O(1)	87.99(7)
		N(4)–Cu(2)–O(1)	103.44(8)
		N(5)–Cu(2)–O(1)	89.94(10)

Synthesis and general characterization of the di- and tri-nuclear complexes

As expected the mononuclear precursors [NiL] **3** and [CuL] **4** effectively function as 'ligand complexes' to yield di- or trinuclear complexes (**5**–**15**). Complexes **3** and **4** are not involved in self-assembling processes. This result is reminiscent of the work concerning quadridentate Schiff base ligands involving an imidazole moiety[27] and possessing similar N_3O donor atom environments, for which it has been found that self-assembling does not occur when benzoylacetone or acetylacetone moieties are involved in the ligands.

FAB^+ mass spectroscopy affords a good characterization of these species since in all cases except for **11** signals directly related to the molecular entity are observed. Indeed, FAB^+ spectra gave intense peaks attributable to $[LCuML''']^+$ cations. In every case, correct ratios of the present isotopes are observed. These results confirm the existence of genuine heterodinuclear complexes along with the absence of the corresponding homodinuclear species in the cases of heteronuclear complexes. Although the FAB^+ spectrum of **7** only shows a peak corresponding to $[LCuNiL^3]^+$, magnetic measurements confirm that a metal redistribution occurs during the reaction. Indeed, the isolated product must correspond to a mixture of $[LCuNiL^3]ClO_4$ and $[LNiCuL^3]ClO_4$ which, obviously, have the same crude formula and the same parent ion in the FAB spectra. We have not succeeded in obtaining a magnetically pure sample. For the trinuclear complexes **12**, **13** and **15**, the signals corresponding to the cationic species (loss of ClO_4) are less intense (7%). On the contrary, the major signal for $[(CuL)_2Mn(bipy)][(ClO_4)]_2$ is situated at $m/z = 726$ (100%) and corresponds to the $[(CuL)_2Mn(ClO_4)]^+$ cation. A peak of lower intensity is observed at $m/z = 627$ (39) which may be attributable to the $[(CuL)_2Mn]$ ion.

In one instance, complex $[LCuCuL^3]ClO_4$ **8**, crystals suitable for an X-ray structural determination have been obtained. A molecular plot is represented in Fig. 3 while relevant bond distances and angles are listed in Table 2. The most significant feature of the structure is the occurrence of a double bridge between the copper ions *via* the oximato group and, more surprisingly, the ketonic oxygen of L. It may be noted that the former bridge links two equatorial positions while the latter is from an equatorial position at Cu(1) to an axial position at Cu(2). The bridging core, Cu(1) [O(1), N(3)–O(3)]Cu(2), is roof shaped since the two Cu(1) and Cu(2) mean equatorial planes make an angle of 104.83(6)°.

Atom Cu(1) is surrounded by the ligand L and displays a square-planar (N_3O) geometry while Cu(2) is in a square-based

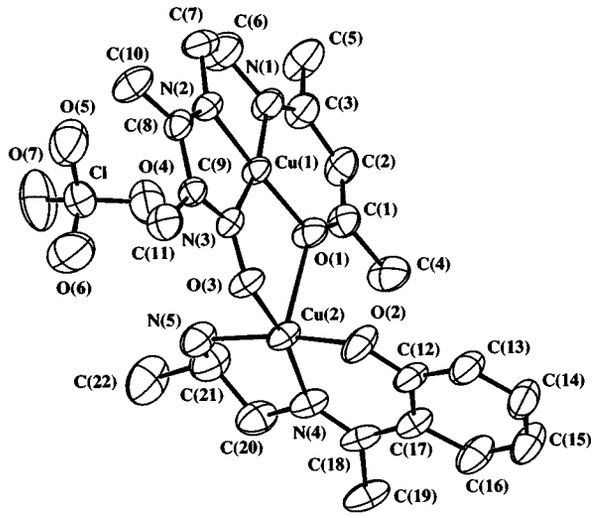

Fig. 3 Molecular plot of **8** with ellipsoids drawn at the 50% probability level

pyramidal environment resulting in a CuN_2O_3 chromophore with an intramolecular copper–copper separation of 3.5071(5) Å. Cu(2) is removed from the mean equatorial plane by 0.174(1) Å in accordance with a (4 + 1) co-ordination mode. The equatorial bond lengths involving Cu(2) lie in the range 1.872(2)–1.985(2) Å and are shorter than the axial bond length [2.524(2) Å]. The metal to ligand bond lengths, in the CuL moiety, are up to 0.1 Å longer than in the nickel complex **3**. This is due to the presence of an antibonding electron in the copper $d_{x^2-y^2}$ orbital.

The Cu(2)L^3 moiety comprises a chiral (*R* or *S*) carbon atom C(21) while the five-membered ring resulting from the chelation of the diamino chain to Cu(2) adopts a gauche (λ or δ) conformation as does the diamino chain of L chelated to Cu(1). In Fig. 3 both cycles have the λ conformations. The methyl substituent grafted on C(21) is remote (r) from the imino nitrogen and adopts a pseudo-equatorial orientation as usually observed for 'half-unit' complexes.[28] Finally we note that the crystal belongs to the space group $P2_1/c$ which is an achiral group so that the cell is heterochiral and optically inactive while, as demonstrated before, each dinuclear unit is chiral. We are led to the conclusion that the four dinuclear units of the cell form two pairs of enantiomers which can be indentified as r*R*λλ and r*S*δδ (the unit represented in Fig. 3 is r*R*λλ).

Finally the shortest intermolecular Cu···Cu separation of 4.4561(3) Å is not large enough to completely discard the possibility of intermolecular interactions.

The UV/VIS spectra of all the complexes display several strong absorptions in the region 450–220 nm. Values of ε of *ca.* 2000 M^{-1} cm^{-1} characterize the 450–400 nm region while ε values >10 000 M^{-1} cm^{-1} are observed between 400 and 220 nm. The d–d transitions of the Ni^{II}, Cr^{III} and Mn^{II} centers are not observable. It has been recently reported that the characteristic absorption of Mn^{II} at *ca.* 410 nm is not detected when the ligand associated with the metal ion contains an aromatic ring.[29]

By contrast, the copper ligand field transitions of complexes **8**–**13** are easily detected at 530 ± 10 nm suggesting that the six complexes would display similar chromophores.

The dinuclear nature of **14** has to be related to several observations showing that, when the co-ordination sphere of a metal ion comprises the tetradentate ligand $[L^2]^{2-}$ associated to a chelating ligand, L^2 adopts a *cis*-β configuration.[20,30–33] This configuration is due to the accommodation of the bidentate ligand completing the co-ordination sphere of the metal ion.

Considering that, in complexes **14** and **15**, the ligand L is likely acting as a chelating ligand, the actual stoichiometry and the consideration of molecular models suggest that the

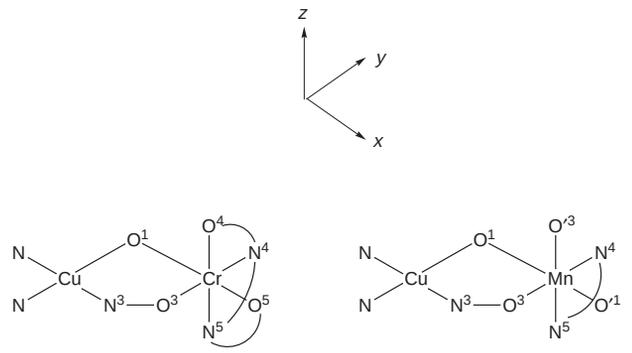

Fig. 4 Schematic representation of the possible structures for **14** and **15**

structures of these species may be derived from that of **8** and schematized as depicted in Fig. 4. It may be noted that the equatorial co-ordination planes around Cr^{III} and Mn^{II} could be defined by O(3), O(4), N(4), N(5) and O(3), O(3′), N(4), N(5) respectively while the related axial positions would be O(1), O(5) and O(1), O(1′) respectively, O(1′) and O(3′) belonging to the second CuL^I entity present in the complex **15**.

Magnetic properties

Complexes **1** and **3** are diamagnetic in accordance with a square-planar geometry. From the susceptibility measurements on powdered samples from 300 to 4 K with a field of 0.1 T, complex **2** is strictly paramagnetic. The data corrected for diamagnetism are well represented by a Curie law $\chi_M T = C$. The *C* value of 0.395 cm^3 mol^{-1} K corresponds to $g = 2.05$. For **4**, $\chi_M T$ is constant from 300 to 20 K and equal to 0.397 cm^3 mol^{-1} K yielding $g = 2.05$. Lowering further the temperature causes a slight decrease of $\chi_M T$ ($\chi_M T = 0.307$ cm^3 mol^{-1} K at 2 K) which is due, most probably, to a weak intermolecular antiferromagnetic interaction.

At room temperature **5** displays a $\chi_M T$ value of 1.179 cm^3 mol^{-1} K corresponding to a moment of 3.09 μ_B which is the value expected for one isolated Ni^{II} paramagnetic ion. Complex **6** is strictly paramagnetic with a *C* value of 0.42 cm^3 mol^{-1} K. The moment at 295 K is equal to 1.77 μ_B confirming that a copper(II) ion is the magnetically active species. A comparison between **5** and **6** shows that Ni^{II} surrounded by the ligand H_2L remains diamagnetic while Ni^{II} co-ordinated to HL^3 is paramagnetic. In this last instance the value of the moment (3.09 μ_B) suggests that Ni^{II} is five-co-ordinate.

In complex **7**, the nickel ion co-ordinated to HL^3 is expected to be paramagnetic. Consequently the magnetic data are interpreted with the expression appropriate for a Cu/Ni-(paramagnetic) pair including the correction term for a 'paramagnetic impurity' [equation (1)][34] where *J* is the inter-

$$\chi_M T = \frac{N\beta^2}{4k}\left[\frac{g_{1/2}^2 + 10g_{3/2}^2 \exp(3J/2kT)}{1 + 2\exp(3J/2kT)}\right](1 - z) + \frac{N\beta^2 g^2 z}{2k} \quad (1)$$

action parameter occurring in the Hamiltonian $-JS_{Cu}S_{Ni}$. The Zeeman factors $g_{1/2}$ and $g_{3/2}$ associated with the doublet and quartet spin states respectively are related to the local factors g_{Cu} and g_{Ni} by the expressions: $g_{1/2} = (4g_{Ni} - g_{Cu})/3$; $g_{3/2} = (2g_{Ni} + g_{Cu})/3$. The symbols *N*, β and *k* have their usual meanings and *z* is the fraction of paramagnetic species. A reasonable agreement [$R = \Sigma(\chi_{obs} - \chi_{calc})^2/\Sigma(\chi_{obs})^2 = 3.2 \times 10^{-4}$] between the observed and calculated data is obtained provided that a relatively large amount of paramagnetic species ($z = 0.12$) is included in the calculation. The resulting parameters are $J = -89$ cm^{-1}, $g_{Cu} = 2.0$ and $g_{Ni} = 2.07$.

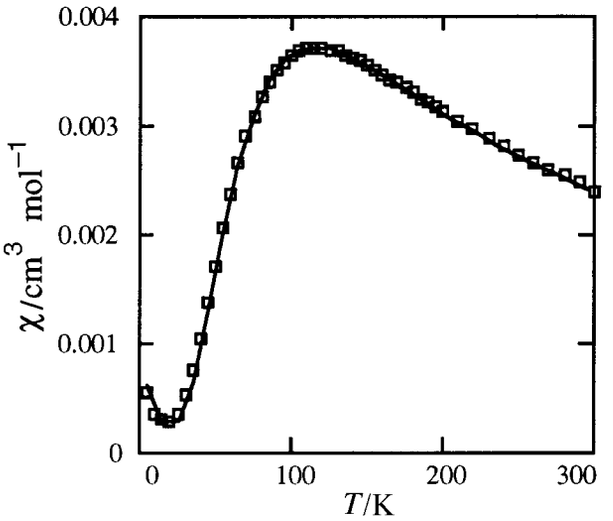

Fig. 5 Thermal dependence of χ_M for **8** at 0.1 T. The full line corresponds to the best data fit

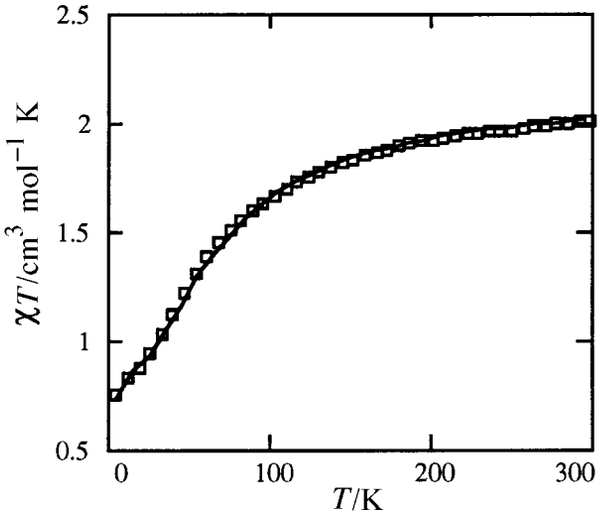

Fig. 6 Thermal dependence of $\chi_M T$ for **14** at 0.1 T. The full line corresponds to the best data fit

As previously noted, the paramagnetic species which has not been detected in the characterization experiments (chemical analysis, mass spectroscopy) is most probably complex **6** which only contains one magnetically active center, the copper(II) ion, and therefore functions as a 'paramagnetic impurity'. The antiferromagnetic behaviour of **7** is not unexpected but the magnitude of the interaction is lower than the values reported in the literature for dinuclear CuNi complexes[13,34–40] ($|J|$ varying from 90 to 205 cm^{-1}).

The three dinuclear Cu^{II}_2 complexes **8**, **9** and **10** display similar magnetic properties. The magnetic behaviour of **8** is represented in Fig. 5 in the form of a χ_M *vs.* T plot. On lowering the temperature χ_M increases, reaches a maximum for $T = T_{max}$ and then decreases tending to zero when T approaches zero. The presence of a maximum can be considered as a signature of antiferromagnetic interaction. Using the relation $|J|/kT_{max} = 1.599$, we may evaluate the magnitude of the interaction *i.e.* $|J| \approx 128$ cm^{-1}. Least-squares fitting of the whole set of experimental data to the Bleaney–Bowers expression[41] derived from the Hamiltonian $H = -JS_AS_B$ leads to $J = -128.7$ cm^{-1} and $g = 2.10$. The fraction of paramagnetic impurity is $z = 0.003$ and the agreement factor $[R = \Sigma(\chi_{obs} - \chi_{calc})^2/\Sigma(\chi_{obs})^2]$ is equal to 1.3×10^{-4}. Similar values are obtained for **9** ($J = -118.5$ cm^{-1}, $g = 2.08$, $z = 0.005$, $R = 2.0 \times 10^{-4}$) and **10** ($J = -93.1$ cm^{-1}, $g = 2.08$, $z = 0.005$, $R = 3.4 \times 10^{-4}$).

Assuming that the three complexes have similar structures (Fig. 3), the decrease of $|J|$ in going from **8** to **9** and **10** could be attributed to an increasing bending of the Cu[O,NO]Cu bridging core due to increasing steric interactions between the two halves of the complexes. These $|J|$ values are rather low with respect to the values generally reported for dinuclear Cu^{II}_2 complexes with double oximato bridges. Values of $|J|$ of the order of 1000 cm^{-1} have been observed but the majority of the reported values lie between *ca.* 600 and 750 cm^{-1}.[3–6,8,10,11,13] The weakness of the interaction in **8**, **9** and **10** may be due at least partly to the incapability of the ketonic oxygen in mediating any appreciable interaction. Indeed the structural study of **8** shows that the bridge joins an equatorial site of Cu(1) to an axial site of Cu(2) which carries, at the best, a very feeble spin density. A J value of -174 cm^{-1} has been recently reported[12] for a dinuclear Cu^{II}_2 complex where the bridging core is restricted to one oximato bridge.

Complex $[LCuCu(HL^6)_2]$ **11** is essentially paramagnetic. It obeys a Curie–Weiss law with $C = 0.761$ cm^3 mol^{-1} K and $\theta = -0.52$ K. The C value is as expected for two independent copper ions. The low θ value implies that a very feeble interaction is operative at low temperatures.

Assuming that **12** is a linear trinuclear complex, the related magnetic data are fitted to [equation (2)]:[42] J and J' being

$$\chi_M T = \frac{N\beta^2 g^2}{4k} \frac{T}{T - \theta} \left[\frac{1 + \exp(J - J'/kT) + 10\exp(3J/2kT)}{1 + \exp(J - J'/kT) + 2\exp(3J/2kT)} \right] \quad (2)$$

respectively the exchange parameters for adjacent and terminal copper ions. The best-fit parameters are $J = -108$ cm^{-1}, $J' = -1.5$ cm^{-1}, $g = 2.04$, $\theta = 0$ and $R = 1.7 \times 10^{-4}$. It may be noted that from 40 to 5 K, $\chi_M T$ remains constant and equal to 0.39 cm^3 mol^{-1} K as expected for an $S = \frac{1}{2}$ ground state without any appreciable interaction between the neighbouring trinuclear units. To avoid overparametrization the exchange integral J' is set equal to -1.5 cm^{-1}, a value resulting from the study of $[Zn(CuL)_2][ClO_4]_2$ **13** ($J' = -1.5$ cm^{-1}, $g = 2.1$ and $R = 2.0 \times 10^{-3}$). The magnitude of the exchange integral between adjacent copper ions $J = -108$ cm^{-1} is of the same order of magnitude as those obtained for the dinuclear complexes **8**, **9** and **10**.

The magnetic behaviour of the dinuclear $Cu^{II}Cr^{III}$ complex **14** is represented in Fig. 6 in the form of the thermal dependence of the product $\chi_M T$. At 300 K, $\chi_M T = 2.01$ cm^3 mol^{-1} K, a value which is smaller than that anticipated for non-interacting Cr^{III} and Cu^{II} ions (2.4 cm^3 mol^{-1} K). As T is lowered, $\chi_M T$ continuously decreases. These two features are consistent with an antiferromagnetic interaction between the two ions leading to an $S = 1$ ground state. The experimental data can be quantitatively interpreted in the 300–5 K temperature range with an expression[43] based on the Hamiltonian $H = -JS_{Cr}S_{Cu}$ [equation (3)]:

$$\chi_M T = \frac{2N\beta^2}{k} \frac{T}{T - \theta} \left[\frac{g_1^2 + 5g_2^2 \exp(2J/kT)}{3 + 5\exp(2J/kT)} \right] \quad (3)$$

N, β, k and J have their usual meanings and θ gauges second-order effects. The Zeeman factors associated with the $S = 2$ and $S = 1$ spins are expressed in terms of the local factors g_{Cr} and g_{Cu}: $g_2 = (3g_{Cr} + g_{Cu})/4$, $g_1 = (5g_{Cr} - g_{Cu})/4$. The best fit parameters are $J = -39$ cm^{-1}, $g_{Cu} = 2.06$, $g_{Cr} = 1.98$, $\theta = -2.0$ K, the agreement factor R being equal to 6×10^{-5}. Below 30 K, the $\chi_M T$ values are smaller than expected (1.0 cm^3 mol^{-1} K) for an $S = 1$ ground state and necessitate the use of a θ value to be correctly fitted. This fact may arise from an intermolecular antiferromagnetic interaction or/and zero-field splitting effects.

The occurrence of an antiferromagnetic interaction in **14** is

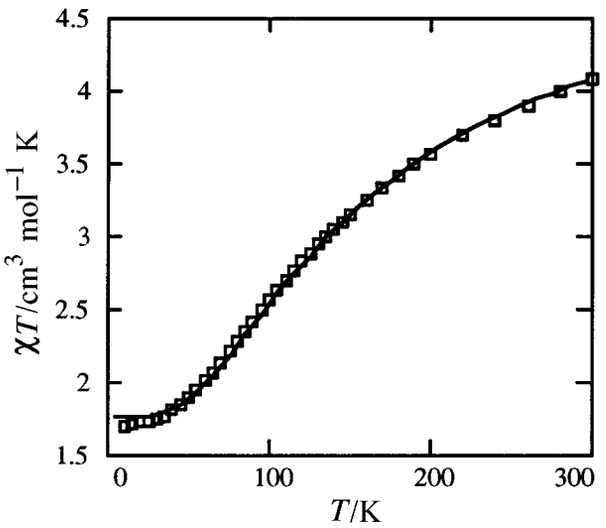

Fig. 7 Thermal dependence of $\chi_M T$ for **15** at 0.1 T. The full line corresponds to the best data fit

unexpected since a survey of the literature[7,13,44,45] shows that most generally, the $Cu^{II}Cr^{III}$ pair has a ferromagnetic behaviour with J values ranging from 25 to 105 cm^{-1}. In these complexes, the equatorial co-ordination planes are coplanar and the ferromagnetism results from strict orthogonality of the magnetic orbitals. As previously noted coplanarity is unlikely for **14** and the whole [LCuCrL²] unit may adopt a very low symmetry, C_s at the best and most probably C_1, which could relax the symmetry requirements for effective overlap of the magnetic orbitals, allowing the antiferromagnetic contribution to be predominant.

The magnetic behaviour of complex **15** is shown in Fig. 7 in the form of the $\chi_M T$ *versus* T. At 300 K, $\chi_M T = 4.08$ cm^3 mol^{-1} K, a value which is lower than that anticipated (5.12 cm^3 mol^{-1} K) for three non-interacting ions (one Mn^{II}, $S = \frac{5}{2}$ and two Cu^{II}, $S = \frac{1}{2}$). As T is lowered, $\chi_M T$ decreases to 30 K and then reaches a plateau with a value of 1.73 cm^3 mol^{-1} K which would correspond to a quadruplet state with $g = 1.9$. These features suggest that intramolecular antiferromagnetic interactions are operative between one Mn^{II} ($S = \frac{5}{2}$) and two Cu^{II} ($S = \frac{1}{2}$) ions. The magnetic data may be quantitatively interpreted using equation (4).[46]

The Zeeman factors associated with the different spin states are expressed in terms of the local factors g_{Mn} and g_{Cu}: $g_{5/2,0} = g_{Mn}$; $g_{5/2,1} = (31g_{Mn} + 4g_{Cu})/35$; $g_{3/2,1} = (7g_{Mn} - 2g_{Cu})/5$; $g_{7/2,1} = (5g_{Mn} + 2g_{Cu})/7$. Least-squares fitting of the experimental data leads to $J = -52$ cm^{-1}, $g_{Mn} = 2.0$ and $g_{Cu} = 2.14$, $\theta = 0$ with an agreement factor equal to 8×10^{-5}.

The behaviour of **15** is consistent with the data reported in the literature[9,12,13,47–49] for di- and tri-nuclear CuMn complexes which, to date, are all antiferromagnetic. In these complexes the two ions are symmetrically bridged by two oxygen atoms from two phenolato groups, two oximato groups or two amidato groups. Generally the resulting $Cu[O_2]Mn$ and $Cu[(NO)_2]Mn$ cores (with associated $|J|$ values up to 72 and 83 cm^{-1} respectively) are more effective in supporting the interaction than the $Cu(OCN)_2Mn$ core ($|J|$ values up to 37 cm^{-1}).[29,36,47–49]

At this stage of the discussion it is tempting to search for a qualitative rationale for the trend and the nature of the exchange interactions within the CuM pairs (M = Cu^{II}, Ni^{II}, Cr^{III} and Mn^{II}). This will be performed within the framework of the model of localized non-orthogonal magnetic orbitals[50–54] and with the basic assumption that the structural drawing represented in Fig. 4 is valid, at least approximately, for all the CuM pairs.

For the Cu^{II} involved in the CuL moiety, the magnetic orbital is of the $d_{x^2-y^2}$ type transforming as a′ (C_s group) and denoted $a'(x^2 - y^2)$ in the following. The unpaired electron around the second Cu^{II}, involved in a CuL^i moiety, is described by an $a'(y^2 - z^2)$ magnetic orbital. For Ni^{II} we have two magnetic orbitals, $a'(y^2 - z^2)$ and $a'(x^2)$. Similarly for Cr^{III} and Mn^{II}, the relevant orbitals are: $a'(xy)$, $a''(xz)$, $a''(yz)$ and $a'(xy)$, $a''(xz)$, $a''(yz)$, $a'(x^2)$ and $a'(y^2 - z^2)$ respectively.

When one of the metal ion has more than one unpaired electron, the experimental J_{CuM} parameter characterizing a CuM pair may be expressed as a sum of components $J_{\mu\nu}$ involving pairs of magnetic orbitals according to $J_{CuM} = (1/n_{Cu}n_M) \sum_{\mu=1}^{n_{Cu}} \sum_{\nu=1}^{n_M} J_{\mu\nu}$ where n_{Cu} and n_M are the numbers of unpaired electrons associated with Cu and M respectively.[54] This expression shows how the magnitude of the interaction is not properly described by J_{CuM} but by the product $n_{Cu}n_M J_{CuM}$ which takes the values: -100 ± 20 cm^{-1} (CuCu), -188 cm^{-1} (CuNi), -117 cm^{-1} (CuCr) and -260 cm^{-1} (CuMn) which point out the relative weakness of the interaction within the CuCu pair.

Let us now consider the expresssions of $n_{Cu}n_M J_{CuM}$ in terms of individual contributions, equation (5).

$$n_{Cu}n_M J_{CuM} = J[a'(x^2 - y^2)_{Cu} - a'(xy)_M]_1 + J[a'(x^2 - y^2)_{Cu} - a''(xz)_M]_2 + J[a'(x^2 - y^2)_{Cu} - a''(yz)_M]_3 + J[a'(x^2 - y^2)_{Cu} - a'(x^2)_M]_4 + J[a'(x^2 - y^2)_{Cu} - a'(y^2 - z^2)_M]_5 \quad (5)$$

The three $J(a'a')$ terms involve pairs of non-strictly orthogonal orbitals. They are expected to afford negative contributions. However we may note that in the two cases, $J(a'a')_4$ and $J(a'a')_5$, overlapping only occurs through one of the two bridging pathways, the ketonic oxygen and the oximato group respectively. This is the main reason why the overall interaction is less effective for the CuCu pair [$J_{CuCu} = J(a'a')_5 \approx -100$ cm^{-1}] than for the CuNi pair [$2J_{CuNi} = J(a'a')_4 + J(a'a')_5 \approx -200$ cm^{-1}]. The term $J(a'a')_1$ deals with orbitals which are situated in the molecular plane and which are not strictly orthogonal to each other since they span the same irreducible representation a′ of the C_s group.§ This term would be responsible for the antiferromagnetic behaviour of the CuCr couple. Indeed the $J(a'a'')_2$ and $J(a'a'')_3$ terms which occur in the expression of $3J_{CuCr}$ concern pairs of orthogonal orbitals which are expected to have positive contributions. However for the intervening $a''(xz)_{Cr}$ and $a''(yz)_{Cr}$ orbitals the molecular plane is a nodal plane and both orbitals are weakly delocalized toward one bridge (O and NO respectively). The net result is that the two $J(a'a'')$ terms may be vanishingly small. As for the CuMn pair, the significant contributions to 5 J_{CuMn} are related to the three $J(a'a')$ terms which are all negative.

It may be noted that these predictions remain qualitatively valid if we take into account a lower C_1 symmetry. In that instance orthogonality does not occur for any pair of intervening orbitals. However lowering the symmetry could increase the possibility of overlap and, eventually, their magnitude with, as a consequence, the increase of the antiferromagnetic interactions.

In conclusion three points of this study deserve a particular attention.

(i) A potentially pentadentate ligand (H_2L) which comprises an oxime group in its structure has been designed and synthesized. Ligand H_2L reacts with Cu^{II} and Ni^{II} ions to yield two

§ This situation contrasts with that previously observed for CuCr complexes of C_{2v} symmetry. In that case, the intervening orbitals, $a_1(x^2 - y^2)_{Cu}$ and $b_1(xy)_{Cr}$ are strictly orthogonal, leading to a ferromagnetic contribution.

$$\chi_M T = \frac{N\beta^2}{4k} \frac{T}{T - \theta} \frac{35g_{5/2,0}^2 + 35g_{5/2,1}^2 \exp(-J/kT) + 10g_{3/2,1}^2 \exp(-7J/2kT) + 84g_{7/2,1}^2 \exp(5J/2kT)}{3 + 3\exp(-J/kT) + 2\exp(-J/kT) + 2\exp(-7J/2kT) + 4\exp(5J/2kT)} \quad (4)$$

types of mononuclear complexes $[M(HL)]^+$ and [ML] [M = Cu^{II} or Ni^{II}] with a N_3OM chromophore, the oxygenated end (OH and O) of the oxime group remaining uncomplexed. Owing to the strong ligand field, the neutral complexes [ML] are not involved in a self-assembling process but can function as 'ligand complexes' to afford homo- and hetero-di- and tri-nuclear complexes.

(ii) The structural study of a dinuclear complex of the [LCu-CuL$''$] type (L$''$ being an auxiliary ligand) shows that the CuL moiety actually behaves as a bridging bidentate ligand for the second copper ion, co-ordinating at an equatorial site *via* the oxygen atom of the deprotonated oxime group and an axial site *via* the ketonic oxygen.

(iii) Generalizing the structure of the Cu[O,NO]Cu core to the $Cu^{II}Ni^{II}$, $Cu^{II}Cr^{III}$ and $Cu^{II}Mn^{II}$ pairs leads to a explanation of the magnetic properties and, more particularly, the unexpected antiferromagnetic behaviour of the $Cu^{II}Cr^{III}$ pair.

Acknowledgements

We thank Dr. A. Mari for his contribution to the magnetic measurements, Dr. A. Bousseksou for providing the fitting program used in this work and Dr. S. Richelme (Service Commun de Spectroscopie de Masse) for her help with the mass spectral measurements.

References

1 J. A. Bertrand, J. H. Smith and P. G. Eller, *Inorg. Chem.*, 1974, **13**, 1649.
2 J. A. Bertrand, J. H. Smith and D. G. van Derveer, *Inorg. Chem.*, 1977, **16**, 1477.
3 D. Luneau, H. Oshio, H. Okawa, M. Koikawa and S. Kida, *Bull. Chem. Soc. Jpn.*, 1990, **63**, 2212.
4 D. Luneau, H. Oshio, H. Okawa and S. Kida, *J. Chem. Soc.*, *Dalton Trans.*, 1990, 2283.
5 K. Matsumoto, S. Ooi, W. Mori and Y. Nakao, *J. Chem. Soc.*, *Dalton Trans.*, 1990, 3117.
6 P. Chaudhuri, M. Winter, F. Birkelbach, P. Fleischauer, W. Haase, U. Flörke and H. J. Haupt, *Inorg. Chem.*, 1991, **30**, 4291 and references therein.
7 Z. J. Zhong, H. Okawa, N. Matsumoto, H. Sakiyama and S. Kida, *J. Chem. Soc.*, *Dalton Trans.*, 1991, 497.
8 P. Chaudhuri, M. Winter, B. P. C. Della Védoca, E. Bill, A. Trautwein, S. Gehring, P. Fleischauer, B. Nuber and J. Weiss, *Inorg. Chem.*, 1991, **30**, 2148.
9 R. Ruiz, F. Lloret, M. Julve, J. Faus, M. C. Munoz and X. Solans, *Inorg. Chim. Acta*, 1993, **213**, 261.
10 R. Ruiz, J. Sanz, F. Lloret, M. Julve, J. Faus, C. Bois and M. C. Munoz, *J. Chem. Soc.*, *Dalton Trans.*, 1993, 3035.
11 R. Ruiz, J. Sanz, B. Cervera, F. Lloret, M. Julve, C. Bois, J. Faus and M. C. Munoz, *J. Chem. Soc.*, *Dalton Trans.*, 1993, 1623.
12 R. Ruiz, F. Lloret, M. Julve, M. C. Munoz and C. Bois, *Inorg. Chim. Acta*, 1994, **219**, 179.
13 F. Birkelbach, M. Winter, U. Flörke, H. J. Haupt, C. Butzlaff, M. Lengen, E. Bill, A. X. Trautwein, K. Wieghardt and P. Chaudhuri, *Inorg. Chem.*, 1994, **33**, 3990 and references therein.
14 B. Cervera, R. Ruiz, F. Lloret, M. Julve, J. Cano, J. Faus, C. Bois and J. Mrozinski, *J. Chem. Soc.*, *Dalton Trans.*, 1997, 395 and references therein.
15 F. Birkelbach, T. Weyhermüller, M. Lengen, M. Gerdan, A. X. Trautwein, K. Wieghardt and P. Chaudhuri, *J. Chem. Soc.*, *Dalton Trans.*, 1997, 4529.
16 P. Pascal, *Ann. Chim. Phys.*, 1910, **19**, 5.
17 K. Everett and F. A. Graf, Jr., in *CRC Handbook of Laboratory Safety*, ed. N. V. Steere, 2nd edn., Chemical Rubber Co., Cleveland, OH, 1971.
18 G. Cros and J. P. Costes, *C.R. Acad. Sci. Ser. 2*, 1982, **294**, 173.
19 J. P. Costes, F. Dahan and J. P. Laurent, unpublished work.
20 F. Lloret, M. Julve, M. Mollar, I. Castro, J. Latorre, J. Faus, X. Solans and I. Morgenstern-Badarau, *J. Chem. Soc.*, *Dalton Trans.*, 1989, 729.
21 C. K. Fair, MolEN, Structure Solution Procedures, Enraf-Nonius, Delft, 1990.
22 G. M. Sheldrick, SHELXS 86, Program for Crystal Structure Solution, University of Göttingen, 1986.
23 G. M. Sheldrick, SHELXL 93, Program for the Refinement of Crystal Structures from Diffraction Data Solution, University of Göttingen, 1993.
24 P. Coppens, L. Leiserowitz and D. Rabinovitch, *Acta Crystallogr.*, 1965, **18**, 1035.
25 A. C. T. North, D. C. Phillips and F. S. Mathews, *Acta Crystallogr.*, *Sect. A*, 1968, **24**, 351.
26 L. Zsolnai, H. Pritzkow and G. Huttner, ZORTEP, Ortep for PC, Program for Molecular Graphics, University of Heidelberg, 1996.
27 T. Nozaki, H. Ushio, G. Mago, N. Matsumoto, H. Okawa, Y. Yamakawa, T. Anno and T. Nakashima, *J. Chem. Soc.*, *Dalton Trans.*, 1994, 2329.
28 J. P. Costes, F. Dahan, J. M. Dominguez-Vera, J. P. Laurent, J. Ruiz and J. Sotiropoulos, *Inorg. Chem.*, 1994, **33**, 3908.
29 C. Mathonière, O. Kahn, J. C. Daran, H. Hilbig and F. H. Köhler, *Inorg. Chem.*, 1993, **32**, 4057.
30 A. M. Sargeson and G. H. Searle, *Inorg. Chem.*, 1965, **4**, 45.
31 P. Coggon, A. T. McPhail, F. E. Mabbs, A. Richards and A. S. Thornley, *J. Chem. Soc. A*, 1970, 3296.
32 M. Calligaris, G. Manzini, G. Nardin and L. Randaccio, *J. Chem. Soc.*, *Dalton Trans.*, 1972, 543.
33 R. B. Lauffer, R. H. Heistand and L. Que, Jr., *Inorg. Chem.*, 1983, **22**, 50.
34 I. Morgenstern-Badarau, M. Rerat, O. Kahn, J. Jaud and J. Galy, *Inorg. Chem.*, 1982, **21**, 3050.
35 S. L. Lambert, C. L. Spiro, R. R. Gagné and D. Hendrickson, *Inorg. Chem.*, 1982, **21**, 68.
36 Y. Pei, Y. Journaux and O. Kahn, *Inorg. Chem.*, 1988, **27**, 399.
37 T. Aono, H. Wada, Y. Aratake, N. Matsumoto, H. Okawa and Y. Matsuda, *J. Chem. Soc.*, *Dalton Trans.*, 1996, 25.
38 M. Yonemura, Y. Matsumura, H. Furutachi, M. Ohba, H. Okawa and D. E. Fenton, *Inorg. Chem.*, 1997, **36**, 2711.
39 E. Colacio, J. M. Dominguez-Vera, A. Escuer, R. Kivekäs and A. Romerosa, *Inorg. Chem.*, 1994, **33**, 3914.
40 E. Colacio, J. M. Dominguez-Vera, A. Romerosa, R. Kivekäs, M. Klinga and A. Escuer, *Inorg. Chim. Acta*, 1995, **234**, 61.
41 B. Bleaney and K. D. Bowers, *Proc. R. Soc. London*, *Ser. A*, 1952, **214**, 451.
42 K. Kambe, *J. Phys. Soc. Jpn.*, 1950, **5**, 48; R. W. Jotham and S. F. A. Keetle, *Inorg. Chim. Acta*, 1970, **4**, 145.
43 Z. J. Zhong, N. Matsumoto, H. Okawa and S. Kida, *Inorg. Chem.*, 1991, **30**, 436.
44 G. Brewer and R. Wang, *J. Chem. Soc.*, *Chem. Commun.*, 1990, 583.
45 Y. Journaux, O. Kahn, J. Zarembowitch, J. Galy and J. Jaud, *J. Am. Chem. Soc.*, 1983, **105**, 7585.
46 O. Kahn, *Molecular Magnetism*, VCH, New York, 1993.
47 K. Nakatani, J. Sletten, S. Halut-Desporte, S. Jeannin, Y. Jeannin and O. Kahn, *Inorg. Chem.*, 1991, **30**, 164.
48 Y. Pei, O. Kahn, K. Nakatani, E. Codjovi, C. Mathonière and J. Sletten, *J. Am. Chem. Soc.*, 1991, **113**, 6558.
49 J. P. Costes, J. P. Laurent, J. M. Moreno Sanchez, J. Suarez Varela, M. Ahlgren and M. Sundberg, *Inorg. Chem.*, 1997, **36**, 4641.
50 O. Kahn and B. Briat, *J. Chem. Soc.*, *Faraday Trans. 2*, 1976, 268.
51 J. J. Girerd, M. F. Charlot and O. Kahn, *Mol. Phys.*, 1977, **34**, 1063.
52 O. Kahn and M. F. Charlot, *Nouv. J. Chim.*, 1980, **4**, 567.
53 M. F. Charlot, J. J. Girerd and O. Kahn, *Phys. Status Solidi B*, 1978, **86**, 497.
54 O. Kahn, *Struct. Bonding (Berlin)*, 1987, **68**, 89.

Received 20*th November* 1997; *Paper* 7/08374B